WOODS HOLE OCEANOGRAPHIC INSTITUTION
Woods Hole, Massachusetts

FC

Reference No. 58-1

An Airborne Flame Photometer and its Use in the Scanning of Marine Atmospheres for Sea-Salt Particles

By A. H. Woodcock and A. T. Spencer

Bubble Formation and Modification in the Sea and its Meteorological Significance
By D. C. Blanchard and A. H. Woodcock

Technical Report No. 15

Submitted to Geophysics Branch, ONR under
Contract Nonr-798(00) (NR-082-124)

January 1958

APPROVED FOR DISTRIBUTION C. O'D. Iselin
C. O'D. ISELIN

AN AIRBORNE FLAME PHOTOMETER AND ITS USE IN THE SCANNING OF MARINE ATMOSPHERES FOR SEA-SALT PARTICLES

By A. H. Woodcock and A. T. Spencer

Woods Hole Oceanographic Institution[1]

(Original manuscript received 25 January 1957; revised manuscript received 22 March 1957)

ABSTRACT

An airborne flame photometer for the identification of large sodium-bearing aerosols from aircraft is briefly described. This instrument is a modified form of a laboratory device which has been used to count sodium particles. A rough calibration of the flame photometer, in terms of the total amounts of sea-salt in marine air, is discussed. Preliminary observations in trade-wind areas are given and an interesting concentration of sodium in cumulus clouds is indicated.

1. Introduction

Evidence of the association of bubbles in the sea with sea-salt nuclei in the air and of the connection between these nuclei and salts in solution in rain waters [see references 1, 3, 16, 18 and 20] has directed our attention to problems requiring more knowledge of the quantities of these nuclei in the atmosphere. In some of these problems an instrument was required which would make possible a rapid scanning from aircraft of the distribution of salt of certain particle-size ranges in the lower layers of marine atmospheres. In these air layers and in the clouds which are often found in them, the difference in the horizontal and vertical distribution of the weight of sea-salt per unit volume of air commonly amounts to several orders of magnitude [17]. Hence, no great instrumental accuracy was initially needed to obtain a useful exploratory tool.

Methods presently available for obtaining the weight of salt per unit volume or weight of air[2] are very slow and laborious. A further objection to most of these methods is that the quantities measured often represent average values along extended air paths due to the necessarily prolonged time required to obtain an adequate sample. Hence these methods are not useful where rapid and rough mapping of the distribution of sodium-bearing particles in the lower layers of marine atmosphere is required.

Soudian [12] and Vonnegut [15] have developed a useful instrument which applies the principles of flame-photometry to the problem of detection of sodium-bearing aerosols. Their instruments are laboratory models, capable of giving relatively instantaneous indications of these aerosols. However, neither author calibrated his instrument in terms of the weight of sodium per unit volume of air nor adapted it for use in aircraft.

The purpose of this article is to describe briefly a flame photometer designed for use in an airplane (see figs. 1 and 2) to discuss its use in conjunction with a different method of measuring airborne salt, and to give some of the first data obtained. This instrument amplifies and records the average voltage developed across the photocell load resistor, which is proportional to the photocell current produced by sodium flashes in a flame. This voltage has been related to the quantity of sea-salt particles in the air, by comparison with direct simultaneous sampling of these salt particles, so that it provides a rapid indication of the weight of sea-salt present. The justification for this comparison of sodium-flash intensity, as represented by the photocell current, to the mass of sea-salt particles in the atmosphere, is to be found in the work of Junge [7, p. 130]. He showed that the ratio of the sodium to the chloride in the giant nuclei in marine air is about the same as this ratio in sea-salts. Hence it was expected that the sodium-flash intensity would be a nearly constant function of the quantity of sea-salt in the air, since the ratio of sodium to total salts in sea-salt is a constant.

2. A brief description of the instrument

The instrument, shown in section in fig. 1, consists of an enclosed gas burner, or torch, into which a mixture of air and propane gas is introduced. The mixture is ignited in flight by a spark which crosses the gap between the center electrode of the spark plug and the outer edge of the burner. Fig. 2 shows the mounting of the flame photometer under the wing of an aircraft.

The flame is viewed by a 1P21 photomultiplier tube through a lens and a multilayer interference filter. This filter has its transmission peak at 5892A, and in-

[1] Contribution number 889 from the Woods Hole Oceanographic Institution. This paper represents the results of research carried out by the WHOI under contract with the Office of Naval Research. Reproduction in whole or in part is permitted for any purpose of the United States Government.

[2] For filtration methods see references [5 and 9], and for impingement methods see references [6, 10, 11 and 19].

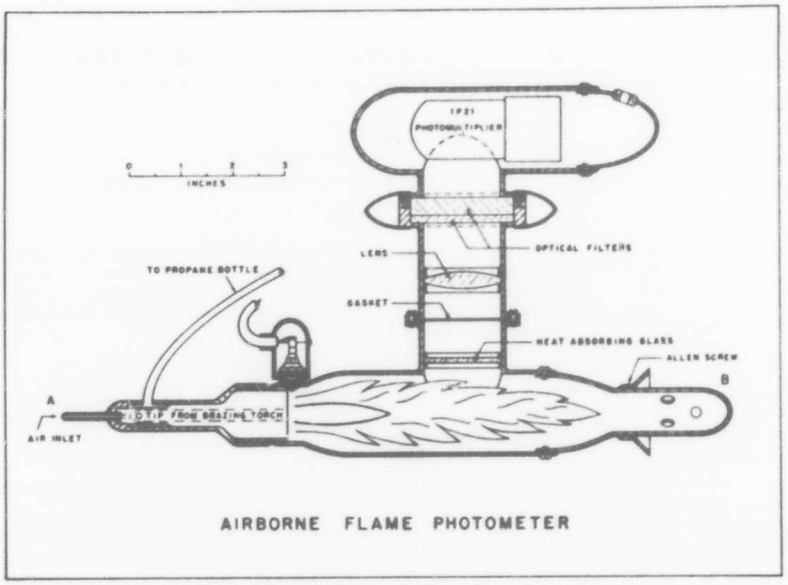

FIG. 1. Schematic drawing of airborne flame photometer.

cludes an additional colored-glass filter for the elimination of side bands.

The output current of the photomultiplier tube is a function of the light from the sodium flashes which occur in the flame as the salt aerosols are heated. This signal from the phototube, after suitable amplification, integration and recording, is related to the airborne salt through comparison with salt-aerosol samples taken and measured by an entirely different technique. This comparison is discussed later in this paper.

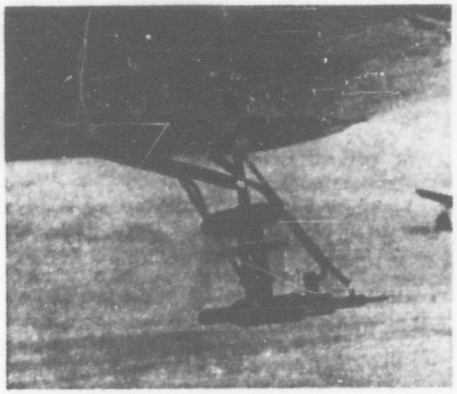

FIG. 2. Photograph of flame-photometer housing mounted under the wing of a small aircraft.

The flow of propane gas to the flame is controlled by a pressure-regulating valve and a floating-ball flow meter. The air enters the burner at A (see fig. 1) at a speed which is controlled by the selected speed of flight. The diameter of the air-intake orifice and the propane-intake pressure required for efficient flame production by the burner were determined by trial in flight at speeds of 70 to 105 mph. It was found that the best flame characteristics for this instrument were obtained with an air speed of about 90 mph, an air-intake orifice diameter of 2.36 mm and a propane flow rate of about 57 gms per hour.

3. Calibration

The sea-salt-particle sampling technique, which was used to indicate the range of usefulness of the output current of the photomultiplier tube as a measure of airborne salt, is one which has been described by Woodcock [16 and 19] and further tested by Twomey [14] and Crozier [4]. This technique involves the exposure to the air of small glass slides and the subsequent measurement with a microscope, under constant relative humidity conditions, of the salt aerosols impinged upon them. When these aerosols are crystalline particles they range in size from about one to ten μ radius and they are known to contain over 90 per cent of the total mass of sea-salts usually present in marine air (Junge, [7] p. 135). The amplifier used with the flame photometer, as presently designed, is sensitive to only the larger of these particles.

In comparing techniques in flight the small glass slides were exposed simultaneously with the operation of the photometer. Over seventy comparative tests have been made in the lower atmosphere (Altitude 200 to 7000 feet) over the sea in the Florida and West Indian regions. During these tests, many factors such as air speed, airplane flight attitude, propane gas flow, phototube supply voltage, etc , which were found to effect the photocell output current, were held reasonably constant

Fig 3 shows the results of these comparative tests. Graph (A) in this figure gives the earlier observa-

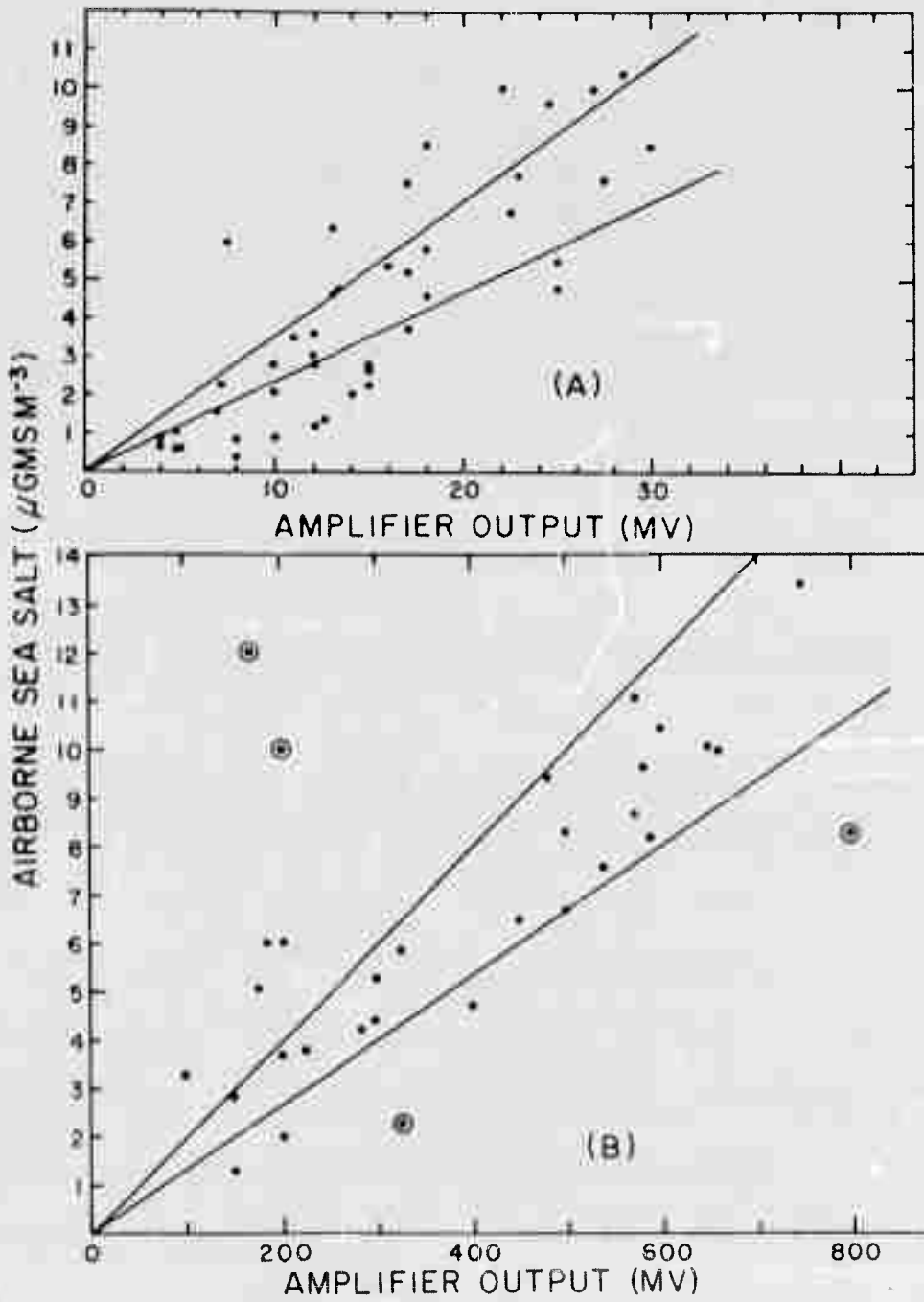

FIG. 3. A comparison of the average photocell output signal, during the periods (30 to 100 seconds) required to obtain the sea-salt particle samples, to the total quantity of sea-salt. The quantities of sea-salt represented by the circled points were derived by extrapolation from a partial sampling with the glass slides of the total range of particle size. These values are therefore subject to the uncertainties of partial sampling. See text for further explanation.

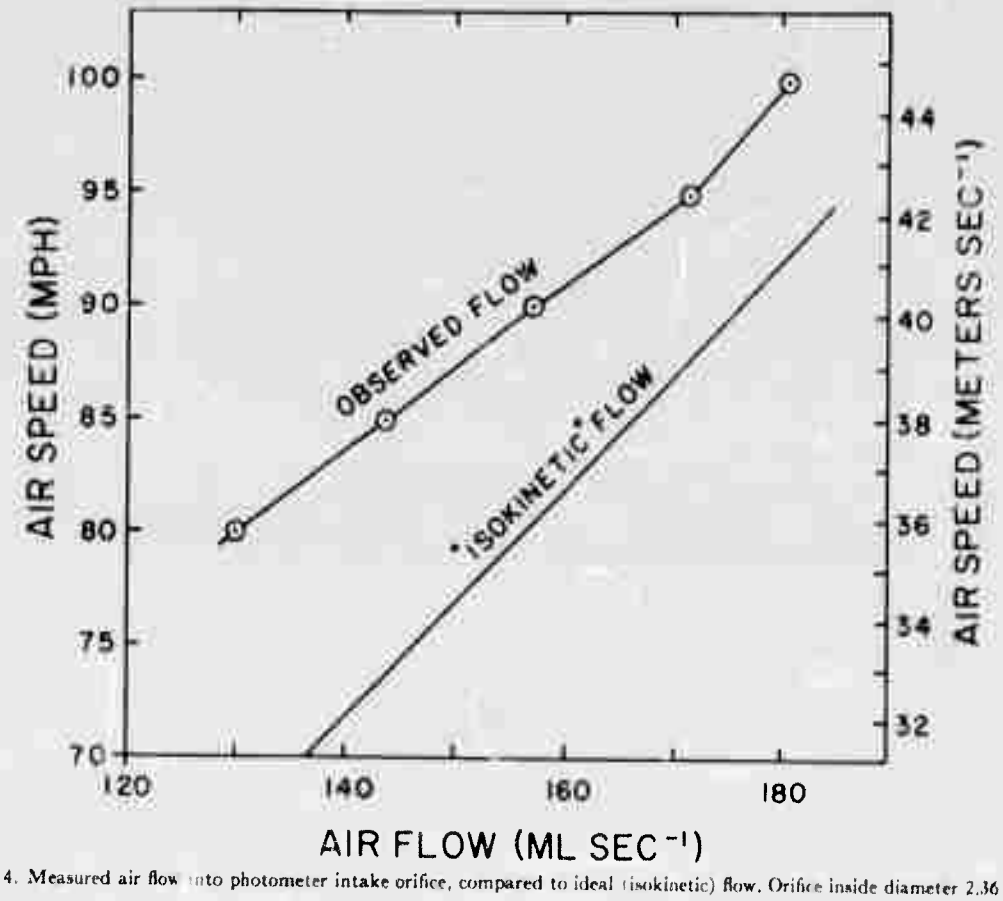

FIG. 4. Measured air flow into photometer intake orifice, compared to ideal (isokinetic) flow. Orifice inside diameter 2.36 mm.

tions made over the ocean east of Pompano Beach, Florida, and graph (B) gives the latest data from the Virgin Island area. The large apparent increase in the voltage on graph (B), as compared to graph (A), is due to increased amplification of the signal in a later model of the instrument. This later model also had an increased sensitivity to the larger sodium flashes. The two diverging lines are introduced among the observed points in order to show the maximum error of the isopiestic method (*i.e.*, ± 20 per cent; see reference [19] p. 181), as applied to the problem of determining the weight of sea-salt particles on the glass slides. These sodium data will be discussed later in this paper.

4. Collection efficiency

May [10] and many other workers have emphasized the importance of "isokinetic" conditions in the intake orifices of aerosol samplers in order to insure that a representative number of particles enter. In other words, with the intake orifice facing directly into the wind, the air speed within the orifice should equal that in the main airstream on the outside. Lower or higher air speeds within the orifice will alter the number of particles which can enter, and hence will alter the apparent concentration of particles in the free air.

In the first exploratory studies of atmospheric sodium particles, no suction was applied to the tail pipe (see B, fig. 1), in order to speed the flow of air through the flame chamber. Hence, internal friction caused the rate of flow of air inside the intake orifice tube (A) to be somewhat less than the air speed of the aircraft. This was demonstrated by placing the instrument in an air stream of a known velocity and measuring the quantity of air passing out of the vent pipe. These quantities were determined by measuring the time required to trap certain volumes of air in a thin-walled rubber balloon. Fig. 4 shows the observed inflow amounts at various air speeds compared to the ideal isokinetic inflow. Note that the measured air inflow at 80 mph was about 17 per cent less than ideal, and at 90 mph about 11 per cent less. These data were obtained with the flame turned off. However, operation of the flame was found to have no measurable effect upon the air-inflow rate at these speeds.

It was sufficient for our present purposes to demonstrate that the amounts of particulate sodium which do enter the orifice and flame, produce a varying sodium-flash signal which in the average is quantitatively related to the varying averaged amounts of sea-salt sampled on the glass slides. It is thought that the

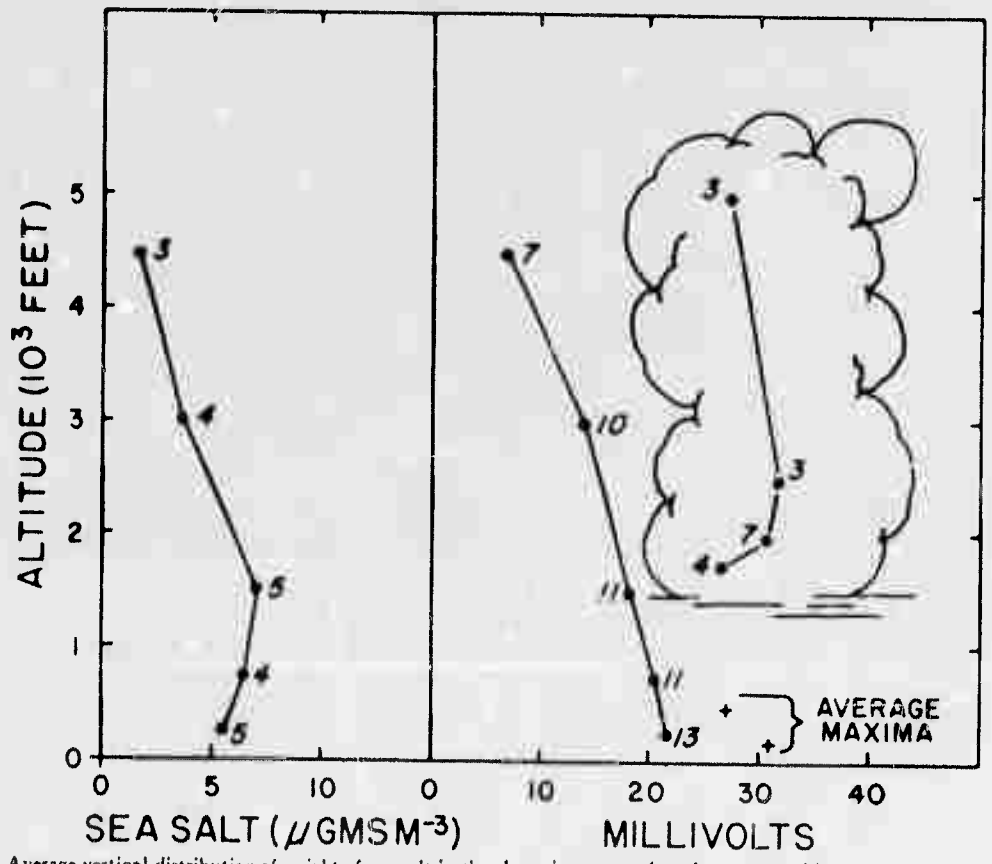

FIG. 5. Average vertical distribution of weight of sea-salt in the clear air compared to the average airborne sodium in the clear air and in cumulus clouds. The sodium is represented by the millivolts output of the amplifier, which is proportional to the photocell current. These measurements were made over the sea, from one-half to two miles east of Pompano Beach, Florida, and during July 22, 23, 24, 25, 27 and 28, 1955. Average local surface winds force 3, ESE. See text for further discussion.

above near-isokinetic-flow values assure a collection efficiency which is quite high enough for the initial exploration discussed here, especially since the outside diameter of intake pipe is so small (2.4 mm) that it would have a high collection efficiency for the particles concerned, from consideration of orifice size alone.

Figs. 5 and 6 show a comparison of the average sodium-flash signal intensity, as indicated by the amplifier-voltage output, to the average quantity of sea-salt found among particles collected on the glass slides. The number of observations averaged in each case is shown near each point. It is apparent on these figures that the differences which occur in the airborne sea-salt and sodium, with increasing altitude, are very similar in trend. This result was expected, since the constancy of the relationship of the sea-salt, among the giant salt nuclei, to the chloride [14 and 19] and to the sodium [6] has been shown.

In figs. 5 and 6 the voltage values are also given for periods when the flame photometer was operated within relatively small nonprecipitating cumulus clouds. Due to the increased mass of the salt particles in the clouds (they become large cloud droplets), the collection efficiency of the photometer intake orifice for these particles would be more nearly unity than for the same particles in the clear air. Thus, these photometer currents obtained within the clouds probably more nearly represent the total sodium present than do the values measured in the clear air.

It will be noted that the average photocell currents in the clouds are similar to but somewhat greater than, the average in the subcloud layer of air. Until further measurements become available, this similarity is tentatively interpreted as showing that the clouds are largely composed of air which has come from the subcloud layer. The higher values obtained in the clouds as compared to the values in the subcloud layer, are thought to result from (1), the tendency for the clouds to be made up of the subcloud air containing the highest amounts of salt (compare cloud voltages on figs. 5 and 6 to the average voltage maxima as shown by the plus signs); (2), a somewhat higher instrumental sampling efficiency in the clouds; and (3), an increase in the concentration (no. per unit volume of air) of the larger salt particles during their growth to large cloud droplets. This third factor is one utilized by Bowen [2] to explain the concentrations of rain-

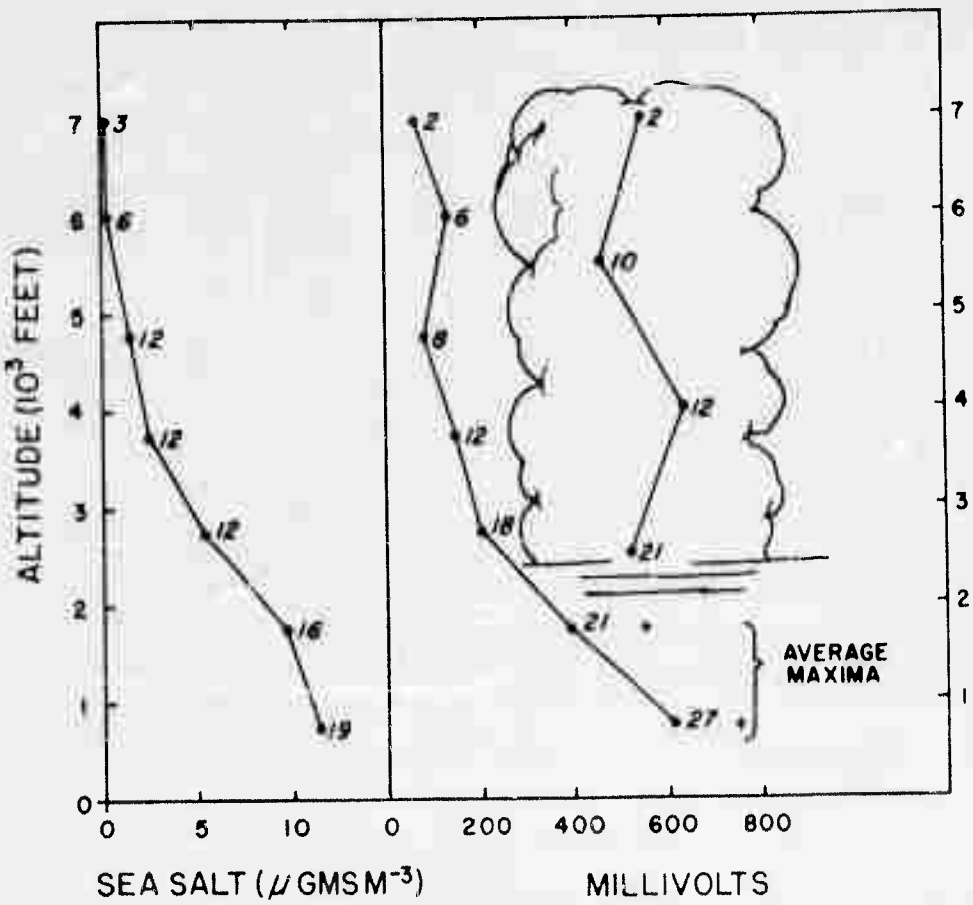

FIG. 6. Average vertical distribution of weight of sea-salt in the clear air, compared to the average airborne sodium in the clear air and in small cumulus clouds. The sodium is represented by the millivolts output of the amplifier, which is proportional to the photocell current. These measurements were made over the sea about five miles southeast of the island of St. Thomas, V. I., and during thirteen days between the dates May 25, 1956 and June 10, 1956. Surface winds force 3 to 5 E to ESE.

drops in clouds, and its application to salt particles is being investigated. It is very unlikely that correction for "sampling efficiency" will significantly alter the cloud sodium values given here. However, until this error is eliminated, these values should be regarded as tentative.

5. Discussion

There is a considerable scatter of the observed points on fig. 3 beyond the ± 20 per cent maximum error of the glass slide method. This is thought to be due in large part to the difficulties of properly integrating the highly variable signal from the phototube, and to variations in the relative mass of salt (or sodium) present in the salt-particle size range sampled by the flame photometer. The variability of the photometer signal during "calibration sampling runs" indicated that the slide samples were averaging a greatly varying quantity. The second of the above factors will be discussed in some detail later. The justification for using the photometer data at this time, despite the above rather large scatter in the calibration values, lies in the close similarity of the changes in the average photometer results, at different altitudes and positions, to changes in the average amounts of sea-salt present (see figs. 5 and 6).

At this stage of its development, the airborne flame photometer is regarded as an exploratory probe in areas where the differences in salt amount are great, and as a device for rapidly "roughing-in" the distributional picture of the sodium-bearing particles in these areas. There is a great difference in the time required to obtain the results by the slide method as compared to the photometer method. For example, the salt data from the glass slides which are shown on fig. 6, required forty hours to produce, while the flame photometer data on this figure are the result of two hours work.

The photometer is especially useful in areas of marked change in aerosol population, such as those which occur while ascending from the subcloud to the cloud and above-cloud layers and while flying through and near cumulus clouds. Where particle size distribution and greater accuracy are required, other methods

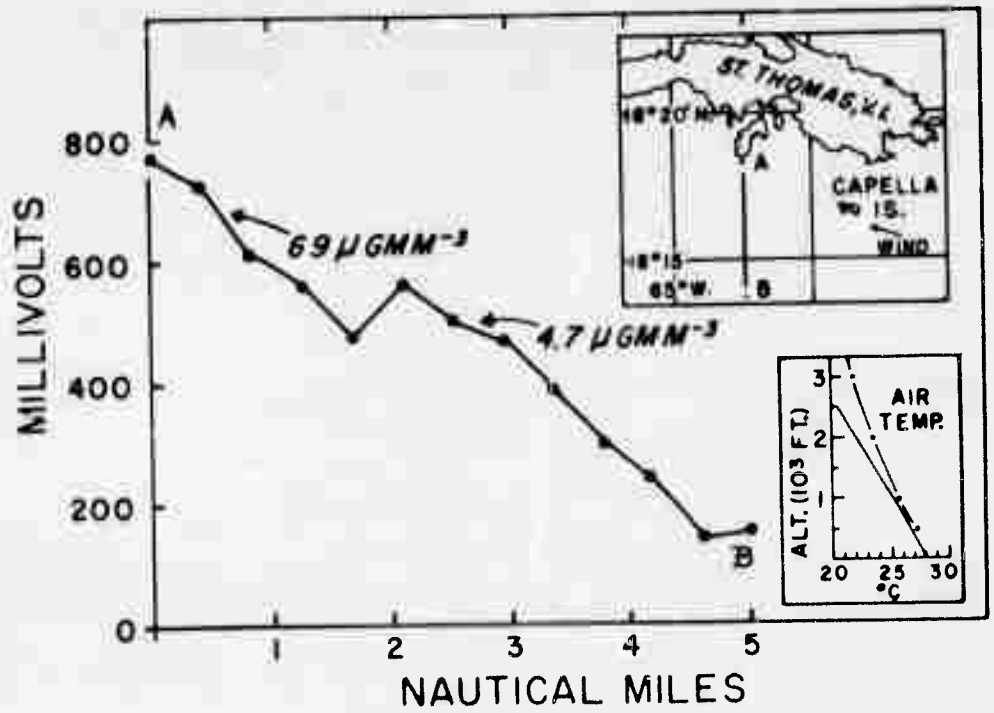

FIG. 7. An example of horizontal differences which occurred in the photocell output signal along the flight line A B (see insert map). The weight values shown represent sea-salt sampled on glass slides a short time later and in the approximate position shown by the arrow marks. Date: June 7, 1956, alt. 500 ft.

may be used. In these cases the photometer is sometimes a valuable supplemental tool. For instance, in some of our problems it is useful to know the maximum quantities of salt present, arriving certain particle size ranges, along a given flight line. Previous methods required that glass sampling slides be exposed as rapidly as possible and at numerous intervals along this line. The "reading" of these many slides was very time consuming and laborious. The continuous record of the photometer makes it possible, however, to scan a flight path and then, upon reversal of course, to use this record as a guide in relocating the areas of maximum salt. Salt samples may then be taken in these areas of interest only, thus saving much time and work.

Fig. 7 shows an example of an interesting horizontal difference in sodium or salt content in the air at constant altitude near an island. This difference, which is not unusual at other levels, is probably due in large part to the convergence of surface air towards the island (caused by island heating) and the consequent subsidence of the relatively salt-free air from higher levels at the off-shore location about five miles south of the island. It may also be due in part to increased wind force near the island causing a greater local production of salt particles by the sea surface (see references [1] and [17] about role of wind in nuclei production).

Though we have used this instrument at low airspeeds on a small aircraft, our experience has indicated that it could be readily adapted for use at the higher speeds of larger airplanes.

In using the flame photometer within clouds, it is reasonable to question the possible effects of cloud water on the flame and on the sodium-flash intensity. It might be supposed that the heat required to vaporize the water on the cloud droplets passing through the flame might, in some cases, so lower the flame temperature that an inadequate amount of heat would remain to heat all of the sodium in each salt particle to incandescence. However, this seems unlikely since the propane burning rate of 67 grams per hour releases from 300 to 1000 times as much heat as that required to vaporize the water found in the average cloud (*i.e.*, from 0.1 to 1 gm m^{-3}). This excess of heat is derived assuming isokinetic flow in the orifice. With this flow, the air passes air through the flame at a rate of about 0.157 liters per second at the airplane speed of 35.8 meters per second (80 mph). The heat of combustion of the propane gas is about 1380 cal per gram.

On several occasions the airplane was directed through "cloud ghosts," or areas in which clouds had recently evaporated leaving an invisible residue of vapor, aerosols and turbulence. These areas also showed the characteristic large increase in sodium-signal intensity which we had found in the visible clouds. Thus it appeared that the increased signal associated with the clouds (see figs. 5 and 6) was not due to some un-

known effect arising from the high state of dilution of the salt particles as cloud droplets.

The effects of changing pressure (altitude) on the gas delivery rate of the commercial "constant-flow valve" used was also measured. The maximum increase in this flow rate due to decreasing pressure with altitude was only seven per cent at 10,000 feet. This increase produces no noticeable effect upon the flame or its sodium-flash signal.

As previously suggested, it is thought that one source of the errors in relating photocell current to individual sea-salt samples taken with the glass slides, (see fig. 3) lies in the changing relative distribution of mass of salt among particles of different sizes. The

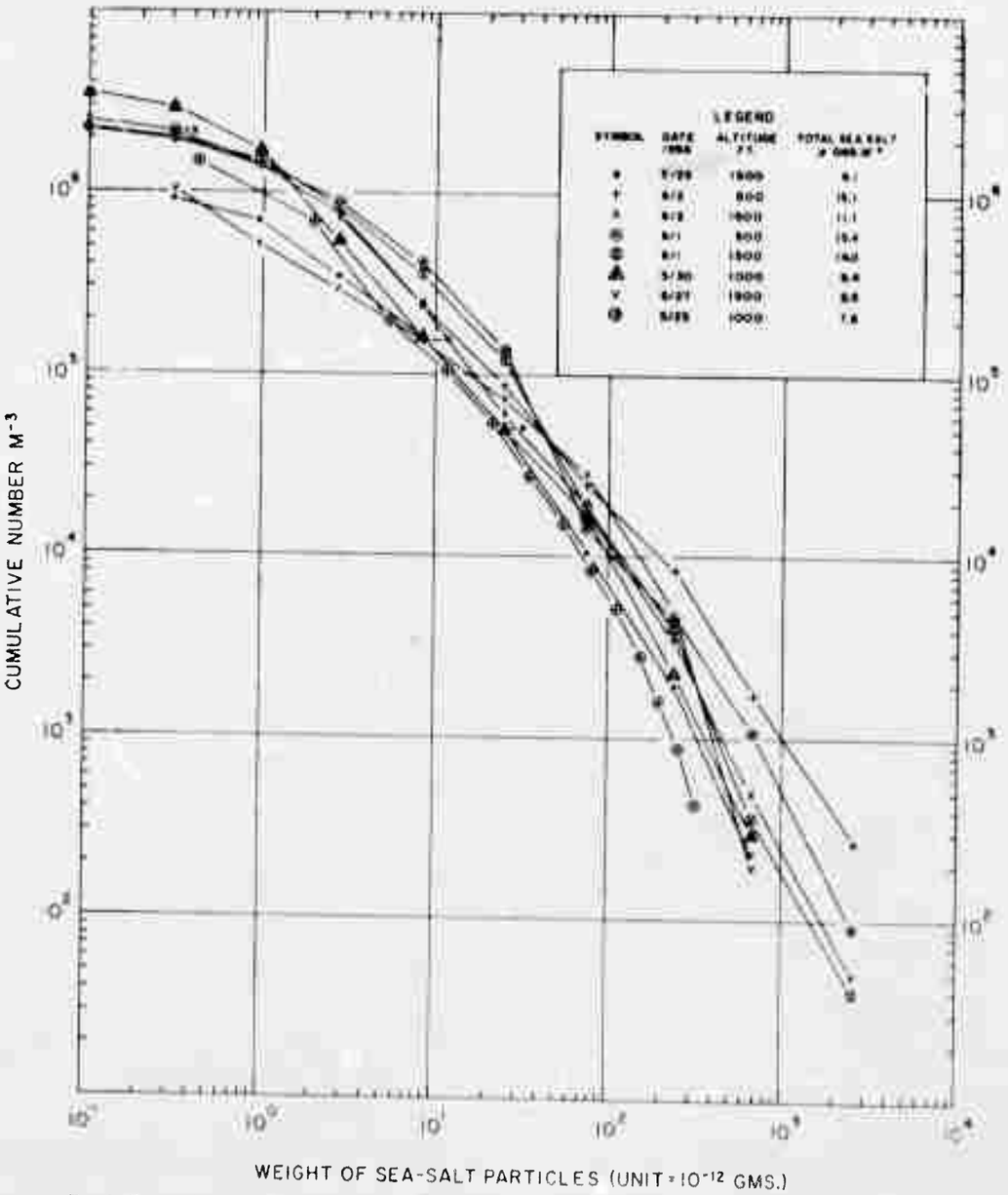

FIG. 8. Cumulative number distribution curves for the samples represented on fig. 9. On this figure and on fig. 9, the symbols represent the lower limiting weight in each weight-range category.

photometer amplifier, as presently constituted, is sensitive to an alternating sodium-flash signal from the larger particles and not to signals from relatively steady sodium light. From a study of the photocell output records from the St. Thomas data, it is known that the major portion of the sodium signal comes from flashes which occur at frequencies of about one per second or less. (There was too little amplification to detect the more numerous weaker flashes.) If we assume that the air entered the intake orifice at a speed of 35.8 m sec^{-1}, the rate at which air passed through the flame is simply the product of the cross-sectional area of the orifice (.04375 cm^2) and the air speed (3.58×10^3 cm sec^{-1}). From this product, which is 0.157 liters per second, and from the spatial distribution of the salt particles, we can determine the particle weight range which produces the flashes of one or less per second. This is done, using the salt-particle distributions derived by the glass-slide technique.

Fig. 8 shows graphically the cumulative number distribution of particles of various weights sampled by the glass slides over the ocean in the Virgin Island area. On this figure one can readily see that the lower limit of the weight range of particles present in numbers sufficient to cause one flash or less per second in 0.157 liters of air (*i.e.*, about 7×10^3 particles or less m^{-3}), is not a constant value. In fact, the "lower limit weight" varies during the several days represented, from about 1×10^{-10} grams to 2.7×10^{-10} gram.[1] Fig. 9, which shows cumulative mass distribution of the salt particles, may be used to determine the relative proportion of the total airborne salt present in nuclei larger than the limiting weight.

As a result of the variable distribution of mass in the weight range sampled by the flame photometer, the instrument probably "sees" a variable proportion of the total salt present. For example, table 1, column 7, shows this varying proportion, expressed as the ratio of the total airborne salt to the salt present in the particles larger than the above-mentioned "lower limit" particle weight. These ratios are derived from the data on figs. 8 and 9 in the following manner. On fig. 8 note that the June 2 salt-particle distribution curve, for the 500-foot level, crosses the limiting number of 7×10^3 particles per cubic meter at a nucleus weight of 270×10^{-12} gram. On fig. 9 the cumulative per cent mass distribution curve for the same day and altitude shows that 34 per cent of the mass of salt was present in particles larger than 270×10^{-12} gram. Table 1, column 7, shows this and other figures for the relative mass of salt present in particles larger than the "lower limit" weight. Correction of the data for this source of error proved inconclusive. This is thought to be due to the small amount of data showing a significantly large difference, and to the obscuring effects of other variables such as the error of the glass-slide method.

[1] The fact that the air entered the orifice at a speed somewhat less than that of the aircraft will alter these values somewhat, but will not alter the basic argument concerning this source of error.

TABLE 1. Showing differences in the ratio of the computed weight of salt which produces the sodium-flash signal, to the total weight of salt in all of the particles sampled by the glass slides. The symbols refer to the data of the six days when the most complete salt-particle samples were taken with the slides (see figs. 8 and 9).

Symbol	Date	Altitude	Airborne sea salt	Particle* weight	Total sea salt in particles equal to or larger than (W)	M2/M1
	1956	ft	M1 $\mu gms\ m^{-3}$	(W) 10^{-12} g	M2 $\mu gms\ m^{-3}$	
⊕	5/25	1000	7.6	90	1.22	0.16
∨	5/27	1500	8.5	190	2.55	0.30
●	5/29	1500	6.1	100	1.58	0.26
△	5/30	1000	9.4	120	1.88	0.20
⊙	6/1	500	15.4	160	3.24	0.21
⊘	6/1	1500	14.0	155	2.24	0.16
+	6/2	500	15.1	270	5.13	0.34
×	6/2	1500	11.1	150	2.55	0.23

* Weight of the smallest particle among the salt nuclei numerous enough to produce one sodium flash a second (i.e., a cumulative number of 7×10^3 particles m^{-3}—see text).

From the above analysis it is seen that an instrument sensitive to only a portion of the range of salt particles entering the orifice should record a signal variability from changing relative mass distribution among these particles. It is clear that a variable signal does not, therefore, necessarily indicate differences in the total mass of salt in the particle size range sampled by the glass slides. Also, there is little doubt that much larger differences in the ratios M2/M1 (see table 1) often occur. Consequently, the present circuit which amplifies the photoelectric cell signal is now being altered to broaden its sensitivity to a greater range of sodium-flash signal frequency. This is expected to remove much of the above source of error.

Alterations are being made in the form of the tail pipe in order to produce a pressure reduction there which will cause the flow rate on the inside of the intake orifice to be equal to that in the free-air stream. The efficiency of the optical system is also being improved. A more detailed description of the airborne flame photometer and of the above improvements is in preparation by the second author.

In the meantime, the present instrument is a useful exploratory tool in those areas of the lower atmosphere where large differences in sodium content are the major features to be studied. We hope to apply the instrument in various field studies. For instance, we would like to know the differences in the salt-aerosol load of the marine air masses moving into "disturbed areas" in the North Atlantic trade-wind system. It is already known that differences in the salt load of the subcloud air of the order of ten to a thousand times are directly related to the speed at which this air has been moving [17]. It has also been shown that these aerosols are

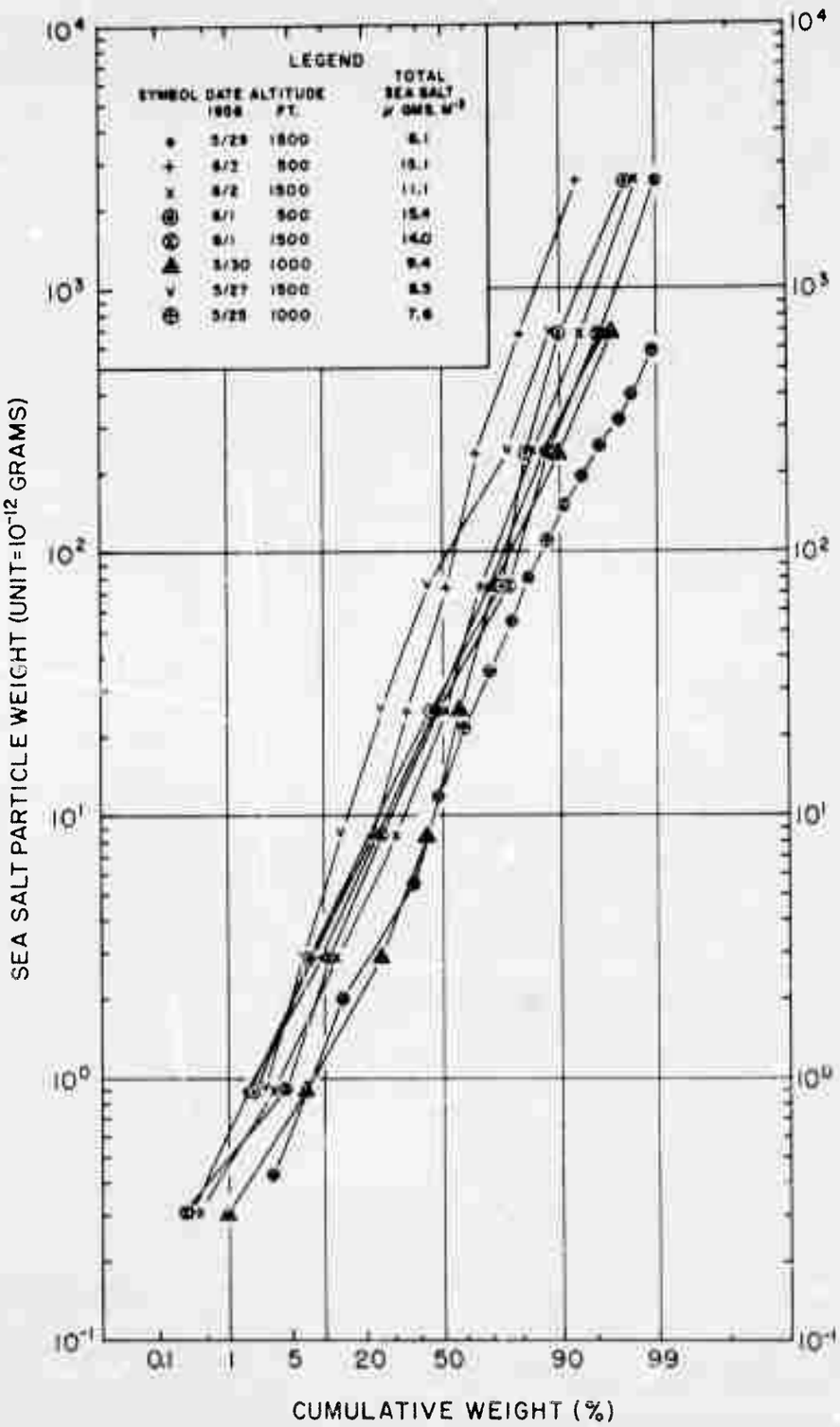

FIG. 9. Cumulative per cent weight-distribution curves, representing atmospheric salt-particle samples taken at the altitudes where, due to more complete sampling, the widest range of particle size was obtained. The sampling location was over the sea in the Virgin Islands region.

probably connected in some way with the rain-forming process [16, 18, and 20]. Large differences in their distribution in air which is moving into a "disturbed area" may be directly connected with the rate and position of release of heat (precipitation) in these areas.

The instrument may also be useful in testing the idea of tradewind cloud growth by the "entrainment" of environmental air. If subsequent measurements continue to show a high relative sodium content in the clouds, it will become necessary to reconsider this idea of cumulus growth. This reasoning follows from the fact that the clear air between the clouds contains relatively small quantities of salt (see figs. 5 and 6 and reference [17]). Hence the extensive mixing of this environmental clear air with cloud air, as pictured in the entrainment hypothesis, should produce a diminishing sodium amount at increasing altitudes in the clouds. This decrease is not revealed by the photometer data thus far. At the present time it seems most likely that the high sodium values in clouds are due to an increase in the number of the salt particles during their growth to large droplets. As previously mentioned, this is one of the questions now being studied with the airborne flame photometer and the glass slide methods.

Acknowledgments.—The authors are indebted to Dr. W. S. Richardson for his valuable suggestions about various aspects of instrument design and to Mr. D. D. Ketchum and Mr. R. G. Walden for their very considerable thought and work in designing and building the amplifying circuits.

REFERENCES

1. Blanchard, D. C., and A. H. Woodcock, 1957: Bubble formation and modification in the sea and its meteorological significance. *Tellus*, **9**, 145–158.
2. Bowen, E. G., 1950: The formation of rain by coalescence. *Australian J. sci. Res.*, **A, 3**, 193–213.
3. Boyce, S. G., 1954: The salt spray community. *Ecological Monographs*, **24**, 29–67.
4. Crozier, W. D., 1954: Errors in the "isopiestic" method for measuring masses of salt particles. *Science*, **120**, 840–841.
5. Jacobs, W. C., 1939: Apparatus for determining the salt content of the air. *Bull. Amer. met. Soc.*, **20**, 38–42.
6. Junge, C. E., 1954: The chemical composition of atmospheric aerosols, I: measurements at Round Hill field station, June–July, 1953. *J. Meteor.*, **11**, 323–333.
7. Junge, C. E., 1956: Recent investigations in air chemistry. *Tellus*, **8**, 127–139.
8. Langmuir, Irving, and K. B. Blodget, 1945: A mathematical investigation of water droplet trajectories. *Gen. Elect. Res. Lab. rpt.*, ATSC Contract W-33-038-AC-9151, pp. 1–47.
9. Lodge, J. P., 1954: Analysis of micron-sized particles. *Anal. Chem.*, **26**, 1829–1831.
10. May, K. R., 1945: The cascade impactor; an instrument for sampling coarse aerosols. *J. sci. Instr.*, **22**, 187–195.
11. Seeley, B. K., 1955: Detection of certain ions in 10^{-10} to 10^{-15} gram quantities. *Anal. Chem.*, **27**, 93–95.
12. Soudain, G., 1951: Realisation d'un compter automatique de noyaux de chlorure de sodium. *Journal Scientifique de la Meteorologie*, **3**, 137–142.
13. Turner, J. S., 1955: The salinity of rainfall as a function of drop size. *Quart. J. r. meteor. Soc.*, **81**, 418–429.
14. Twomey, S., 1954: The composition of hygroscopic particles in the atmosphere. *J. Meteor.*, **11**, 334–338.
15. Vonnegut, B., 1952: Counting sodium-containing particles in the atmosphere by their spectral emission in a hydrogen flame. *Occasional report, Project Cirrus, General Electric Co.*, No. 38, 1–18.
16. Woodcock, A. H., 1952: Atmospheric salt particles and rain drops. *J. Meteor.*, **9**, 200–212.
17. Woodcock, A. H., 1953: Salt nuclei in marine air as a function of altitude and wind force. *J. Meteor.*, **10**, 362–371.
18. Woodcock, A. H., and D. C. Blanchard, 1955: Tests of the salt-nuclei hypothesis of rain formation. *Tellus*, **7**, 437–448.
19. Woodcock, A. H., and Mary M. Gifford, 1949: Sampling atmospheric sea-salt nuclei over the ocean. *J. marine Res.*, **8**, 177–197.
20. Woodcock, A. H., and W. A. Mordy, 1955: Salt nuclei, wind and daily rainfall in Hawaii. *Tellus*, **7**, 291–300.

Särtryck ur Tellus nr 2, 1957

SVENSKA GEOFYSISKA FÖRENINGEN

VOLUME 9, NUMBER 2 **Tellus** MAY 1957

A QUARTERLY JOURNAL OF GEOPHYSICS

Bubble Formation and Modification in the Sea and its Meteorological Significance

By D. C. BLANCHARD and A. H. WOODCOCK[1]

Woods Hole Oceanographic Institution

(Manuscript received November 2, 1956)

Abstract

It is believed that the vast majority of the airborne salt nuclei arise from bursting bubbles at the air—sea water interface. Four natural mechanisms for the production of these bubbles have been studied. These are whitecaps, rain, snow and supersaturation of the surface waters of the sea due to spring warming. The bubble spectra from whitecaps and snowflakes have been measured and semi-quantitative and qualitative observations have been made on the bubble spectrum produced by raindrops. No evidence of bubble production by spring warming has been obtained.

All of the measurements show that a majority of the bubbles are < 200 microns diameter and, in the case of bubbles from snowflakes, < 50 microns. In the vicinity of a breaking wave the bubble production rate is about 30 cm^{-3} sec^{-1}.

Due to the effects of surface tension in increasing the bubble internal pressure all bubbles < 300 microns will go into solution even at sea water air saturations of 102 percent. Bubbles < 20 microns will go into solution at saturations up to 115 percent! The solution time for small bubbles of about 10 microns is about 10 sec and is not markedly affected by the water saturation percentage.

It is concluded that the effects of the rate of solution of bubbles in sea water can, under some conditions, play a significant role in modifying the initial bubble spectrum. This, in turn, should influence the spectrum of airborne nuclei.

1. Introduction

It seemed evident from the work of WRIGHT (1940) and KÖHLER (1941) that large salt particles were playing an active role in visibility changes in the lower atmosphere and perhaps in cloud formation as well. It was not until the work of WOODCOCK (1949 and 1952) however that the existence of these particles throughout the entire subcloud and cloud layers in marine air was shown. CROZIER and SEELY (1950), TWOMEY (1955), and BYERS (1955) have demonstrated that significant concentrations of these aerosols exist in air masses that had traveled many hundreds of miles over land. A consideration of the potential importance of these particles in the mechanism of rainfall production is, therefore not limited to clouds over oceanic areas. LUDLAM (1951) and BOWEN (1950) have both shown, on a theoretical basis, that hygroscopic particles of the size of the salt nuclei found in the atmosphere are sufficiently large to grow rapidly into raindrops, by the process of coalescence with smaller cloud droplets. Recently WOODCOCK (1952) and WOODCOCK and BLANCHARD (1955) have compared the raindrop spectrum and the rainwater chlorinity with the salt nuclei spectrum in the sub-cloud layer. These results have suggested that each salt nucleus becomes a rain-

[1] Contribution Number 875 from the Woods Hole Oceanographic Institution. This paper represents the results of research carried out by the Woods Hole Oceanographic Institution under contract with the Office of Naval Research. Reproduction in whole or in part is permitted for any purpose of the United States Government.

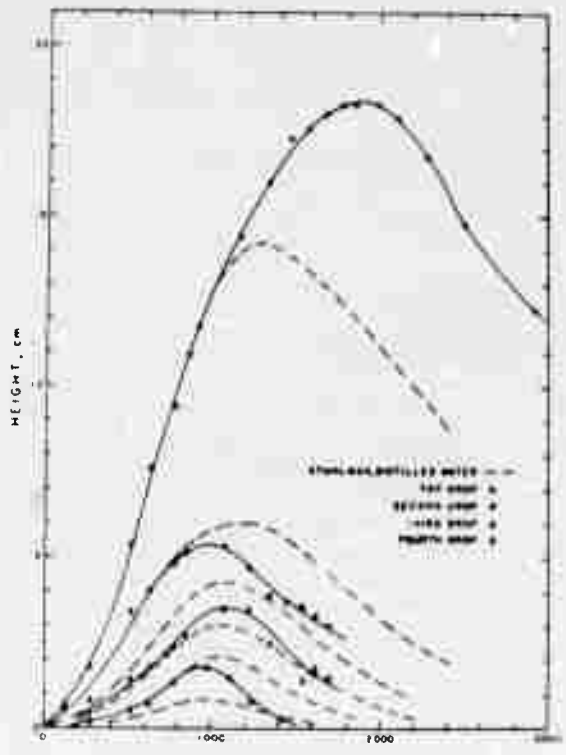

Fig. 1. This illustrates the heights of ejection of the several drops from the jet of a bubble bursting in sea water. STUHLMAN's (1932) findings are shown for the top drop from bubbles bursting in distilled water.

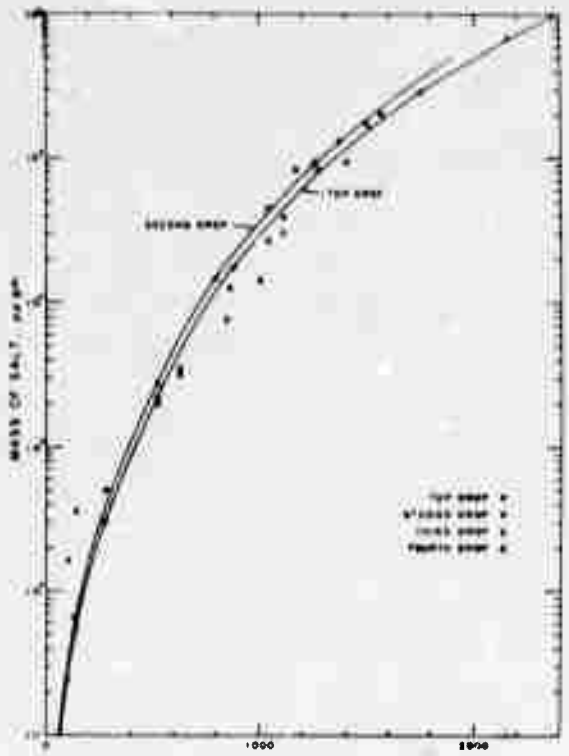

Fig. 2. This indicates the mass of salt contained in the drops that are ejected from bubbles bursting in sea water. This figure combined with Fig. 1 will give the ejection heights and drop size as a function of bubble diameter for the top four of the drops that evolve from the jet of a bursting bubble.

drop and that any modification of the sea salt spectrum will change the raindrop spectrum and possibly the manner of rainfall production. In the present paper we shall discuss the natural methods of production of salt particles at the sea surface and show that these methods should, in fact, be capable of modifying the existing salt nuclei spectrum.

The source of the airborne salt particles is, of course, the sea. Some of the first attempts at measurement of the salt spectrum were made near the sea surface by OWENS (1926). COSTE and WRIGHT (1935) showed that salt nuclei could be produced by spraying sea water and ALIVERTI and LOVERA (1939) produced small particles by bubbling air through sea water. KÖHLER (1941) forced air through sea water and found salt nuclei produced down to a radius of about 0.5 micron. None of these investigators, however, was greatly concerned with the exact mechanism of nuclei production; whether it was by mechanical disruption of the water by breaking bubbles or some other process. In 1948 Woodcock suggested that salt particles were ejected into the air from breaking bubbles by a mechanism first suggested by STUHLMAN (1932). BOYCE (1951) carried out an experiment that suggested that relatively few salt particles were produced by the mere mechanical "tearing" of the water in a breaking wave but that a significantly greater number could be produced a few seconds later when the bubbles resulting from the wave action had burst at the sea surface. A high-speed photographic study (KIENTZLER ET AL., 1954) confirmed the mechanism of the ejection of droplets from a breaking bubble (STUHLMAN 1932). The photographs indicate the manner in which small airborne droplets evolve from the vertical water jet which forms upon collapse of the bubble cavity. As seen in Fig. 1 and Fig. 2 the heights to which these droplets are ejected and their size is a function of the bubble diameter. The heights were

obtained with the use of a cathetometer and the bubble size determined from measurements of the buoyant force from a known number of bubbles collected in a small inverted glass hemisphere. The size of the ejected drops was determined by catching them on glass slides and exposing them to an atmosphere of known humidity. The resulting drop size could then be used to compute the sea salt content and thus the original size of the drop.

MASON (1954), MOORE and MASON (1954) and KNELMAN ET AL. (1954) found that the breaking of the bubble film produces small drops. It appears that the production of droplets by this mechanism is limited to the larger bubbles and any evaluation of their importance in modifying the salt particle spectrum over the sea must await an experimental study on the actual bubble spectrum. This point will be discussed later in the paper.

The foregoing work suggests that it is the breaking bubble at the sea surface that is responsible for the production of the atmospheric salt particles. In the next section the variation in bubble production by wave action and precipitation will be discussed.

2. Bubble Production at the Sea Surface

A. Wave Action

It is well known that increasing winds cause a proportionate increase in the production of "whitecaps" at the sea surface. These whitecaps produce bubbles in the sea which, when they break at the surface, produce airborne salt nuclei. Therefore a direct relation should exist between wind force and the concentration of airborne salt. This in fact has been found at deck levels by FOURNIER D'ALBE (1951), MOORE (1952) and at cloud levels by WOODCOCK (1953) Woodcock found that the weight concentration of sea salt at cloud base levels was increased by a factor of about ten when the wind force changed from three to seven.

It might be well to point out that in strong winds the effective area over which bubbles are breaking is appreciably greater than that covered by the obvious breaking wave. For a minute or more after the wave breaks the water in the immediate vicinity appears cloudy without the presence of a heavy foam patch on the surface. This cloudy appearance is caused by the myriads of bubbles that are formed by the breaking wave. The persistence of the cloudy region signifies that the bubbles are small and thus slow in reaching the surface or that they have been carried far beneath the surface. Presumably the stronger the wind the more bubbles are produced and the deeper they are carried by the turbulent motions of the sea. Observation indicates that little or no coalescence occurs amongst the bubbles when they reach the surface. If this surface is clean the bubbles will break immediately. In the laboratory, experiments have been carried out by bubbling air through fine frits placed a few cm beneath the surface of the water. A rapid coalescence of bubbles occurs on the surface of fresh water but this is not observed in the case of sea water. Even though they are packed tightly at the surface the individual bubble bursts seem unaffected by the adjacent bubbles. It appears safe to assume that bubbles produced in the sea by wave action will in most cases burst individually at the sea surface and not coalesce.

The device that was used to determine the bubble spectrum produced by breaking waves consisted of a small ($9 \times 6 \times 2$ cm) box with one of the 9×6 cm sides transparent. A grid of lines was inscribed on this transparent side of the box, the opposite side being removable. Just prior to making a bubble count the box was completely filled with sea water and the removable side securely attached. The box was then placed, transparent side up, just beneath the sea surface in a region where breaking waves had left the sea cloudy with bubbles. The removable side (now the bottom) was slipped aside for a known time interval during which bubbles were free to rise into the box and become entrapped against the underside of the transparent top. The bottom was then securely attached to prevent leakage and the box removed from the water. Using a scale and a magnifying lens, the bubble spectrum, divided into appropriate size ranges, could be obtained.

A brief consideration of the energies involved showed that there was no danger of a flattening of the bubbles against the underside of the glass. For bubbles < 500 microns diameter the surface free energy is at least 400 times as great as the gravitational energy. Any bubble surface distortion, which must arise from the gravita-

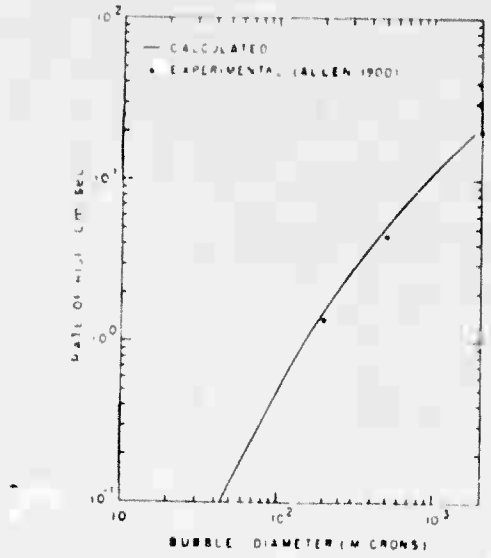

Fig. 3. The rate of rise of air bubbles in water. The calculated values are for sea water while the experimental ones are for fresh water.

tional energy, will be opposed by the surface free energy which, of course, tends to a minimum. It is apparent from the above considerations that the bubble surface distortion could not exceed 1/400 or 1/4 of one percent and thus the diameter will not undergo any significant change.

The bubble density or number per unit volume of water is easily obtained by dividing the number found in each size range by the area that was counted, the time of exposure and the rate of rise of the bubble in water. The size ranges were in 100 microns steps up to 500 microns. The rate of rise of the bubbles in each size range was assumed to be represented by the rising speed of the average sized bubble, with the exception of the first size range, where the representative rise speed was that for a 75 micron diameter bubble.

The rate of rise of bubbles in water may be calculated in the following manner. The general expression for the frictional retarding force is

$$f = 6\pi n r v \left(\frac{C_d \cdot R}{24}\right) \qquad (1)$$

where n is the viscosity of the water; r, the bubble radius; v, the velocity of rise; C_d, the drag coefficient; and R, the Reynolds number. This expression can be derived in a straightforward manner from Stokes' Law and the fundamental relation between actual drag and impact drag. Now the buoyant force on the bubble is

$$f_b = 4/3\,\pi r^3 g\,(\varrho_w - \varrho_a) \qquad (2)$$

where g is the gravitational acceleration and ϱ_w and ϱ_a the density of sea water and air, respectively. At the terminal or steady state velocity of the bubble (2) must equal (1). By equating these expressions and then substituting for v in terms of the Reynolds number

$$v = \frac{nR}{2\varrho_w r} \qquad (3)$$

and letting $\varrho_a << \varrho_w$ we obtain

$$r^3 = \frac{9n^2}{4\varrho_w^2 g} \quad \frac{C_d R^2}{24} \qquad (4)$$

C_d has been found to be a function of only the Reynolds number (GOLDSTEIN 1938) so, given any value of R, C_d may be obtained and (4) can be solved for r. With this value of r and R, (3) may be solved for the rate of rise v. In like manner a number of r versus v tabulations can be determined and a graph drawn. Figure 3 shows the calculated values plus some experimentally observed rise velocities (ALLEN, 1900). Allen's values were used for the bubble density calculations in this section while the calculated values outside of Allen's observations were used for the discussions in

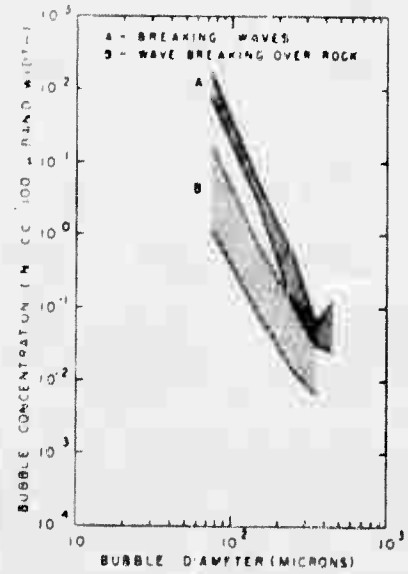

Fig. 4. The bubble concentration (cc^{-1} per 100 μ band width) in sea water produced by breaking waves or whitecaps.

the latter part of the paper. Stokes' law will apply for bubbles below about 110 microns diameter.

Figure 4 summarizes the experiments made on the bubble spectrum from breaking waves. All the experiments were carried out during the summer months on a beach near our laboratory where the water temperature was about 21° C. The hatched region A shows the limits of bubble density for six separate experiments conducted during a 2-hour interval at a time when fresh onshore winds were causing the waves to break about 15 meters from shore. The bubbles were obtained by wading some 5 meters out and exposing the sampling device already described for 2 seconds at a depth of about 10 cm. The measurements were made a few seconds after the breaking wave had passed. It was necessary to wait these few seconds to allow the relatively few bubbles of several mm diameter to rise to the surface. These large bubbles produced undesirable coalescence in the collecting box. It is realized that this method discriminates against the mm sized bubbles but they are present in far fewer numbers then the bubbles < 500 μ. The bubble spectrum in these experiments was determined out to a diameter of 750—1,500 microns but, as the size interval was 500 microns in this region, the values could not, without approximation, be plotted on Fig. 4. Had this been done the extension of region A and B would have continued with about the same slope as it has at present. Region B, an order of magnitude less than A, represents the spread of six determinations of the bubble spectrum found on the lee side of a rock over which the waves were breaking. The wind was not as strong as it was during the former measurements.

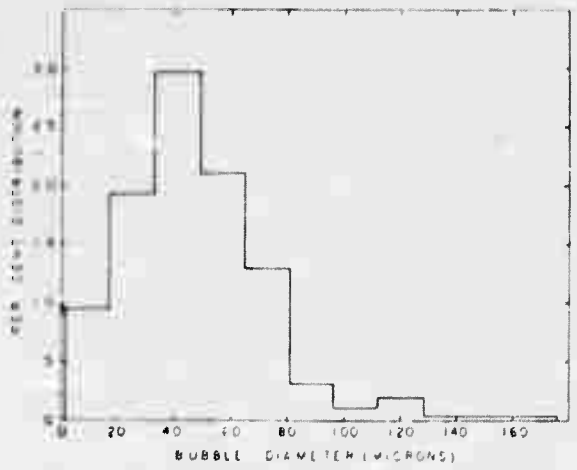

Fig. 5. The size distribution of bubbles, rising from a snowflake cluster melted in sea water.

B. Snow

Among the natural sources of small bubbles in surface waters of the sea we have found that snowflake clusters are very significant. These bubbles, which are released as the snowflakes melt, are readily observed by allowing a snowflake to fall into a small beaker which is brimming full of sea water, and then quickly placing a clean glass cover-slip over the water in order to trap the bubbles. From fifty to several hundred bubbles were observed to rise and collect under the cover-slip as single flakes melt. Figure 5 shows the size distribution of some three hundred of these bubbles, which were measured with a low-power microscope using an eyepiece micrometer.

While making these size measurements, which required perhaps 10 minutes, it was observed that bubbles smaller than about 30 μ diameter were slowly becoming smaller and that bubbles 50 μ or larger were growing. Thus the size distribution shown on Fig. 5 is only qualitatively correct, serving here only to emphasize the capabilities of snow in producing (or causing to be produced) a wide range of size among very small bubbles. Since, during the observation period, the small bubbles were becoming smaller and the large bubbles were becoming larger an increase in the size range with time occurred. This means that the initial bubble size distribution, present immediately after the flakes melted, was more limited in range than is shown in Fig. 5. The effects of time of immersion in altering a given initial bubble population depends upon a number of factors, such as depth of water, partial pressure of air in solution, etc. These and other factors are discussed at length in Section 3 of this paper.

C. Raindrops

The production of bubbles and nuclei by the impact of raindrops on the sea surface is a complex problem. It has been found that bubbles, produced directly and indirectly through the impact of raindrops, can produce

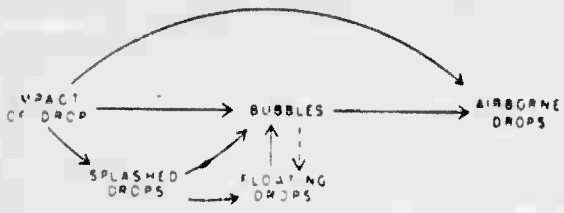

Fig. 6. A diagrammatic sketch of the methods of production of airborne drops by the impact of a fresh-water drop on a sea water surface. The dotted arrow indicates that floating drops are associated primarily with the collapse of the larger, less numerous bubbles.

nuclei. Before an attempt is made to describe these bubble-production methods in detail, and to show how they vary over the raindrop spectrum, it might be well to consider them in schematic form as shown in Fig. 6. It can be seen that the nuclei are produced either directly from the impact of the drop, or from bubbles produced as a result of the impact. The bubbles are produced by (1) direct impact of the raindrop on the sea surface, (2) splashed drops resulting from the impact, and (3) drops that momentarily remain floating on the sea surface.

Observations on the splashing of water and production of bubbles by simulated raindrops were made by visually observing, with suitable lighting, the behavior of freshwater drops on impact with a sea water surface. The drops were allowed to fall from a sufficient height to insure terminal velocity. The splashed drops and the smallest bubbles were easily visible in a parallel beam of light from a microscope lamp, using a suitable black velvet background. An estimate of the size of the bubbles and drops was made by applying Stokes' Law to the rate of rise and fall, respectively.

The direct production of bubbles by raindrops is a function of raindrop size. Small drops of the order of 0.4 mm diameter will produce 2 or 3 bubbles of about 50 μ diameter that are carried only 1—3 mm beneath the surface. The production of bubbles increases rapidly with drop size as a 2.2 mm drop was observed to produce from 50—100 bubbles that were often carried down in a vortex ring to depths of 2—4 cm. The vast majority or these bubbles appeared to be under 50 microns diameter. On occasions it appeared that the vortex ring of bubbles formed not at the moment of impact of the drop with the water but at the collapse of the water column that rises from the bottom of the impact cavity. This is quite plausible, for the remarkable photographic work of WORTHINGTON and COLE (1897) shows this water column, and they remark about the vortex ring that it forms upon collapse. They make no mention of bubbles in the vortex ring but they probably passed undetected as only the closest scrutiny will discover them. With increasing drop size an increase in number of bubbles was observed, although the bubble size was predominantly the same. Drops of 3 mm produced 100—200 bubbles while 4.7 mm drops produced an estimated 200—400 bubbles (see Fig. 7). The larger drops also produce several bubbles of about a mm diameter. With increasing drop size the vortex motion of the bubbles plus the depth of penetration decreased. The bubbles from drops of 4.7 mm were carried down less than 2 cm but eddy motions distributed bubble clusters some 3 cm horizontally. These bubbles would go rapidly into solution or grow depending upon whether the sea water was considerably under- or oversaturated, respectively. This, of course, will modify the bubble spectrum which in turn will affect the salt nuclei that are produced when the bubbles burst. This solubility effect of the bubbles is considered in some detail later in the paper.

The indirect production of bubbles by raindrops occurs when the drops produced by the splash of the raindrop fall back into the sea. As this method of bubble production depends

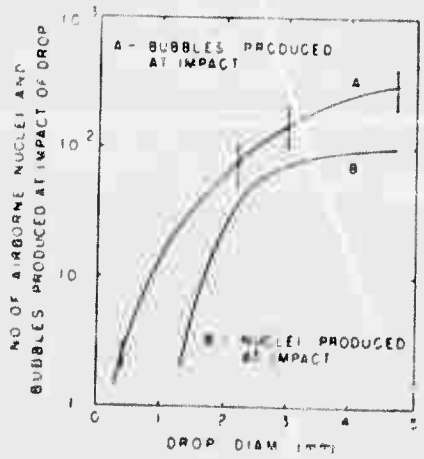

Fig. 7. Curve A represents the number of bubbles produced by the impact of a fresh-water drop on a sea water surface. Curve B represents the direct production of nuclei by the same drop at the moment of impact.

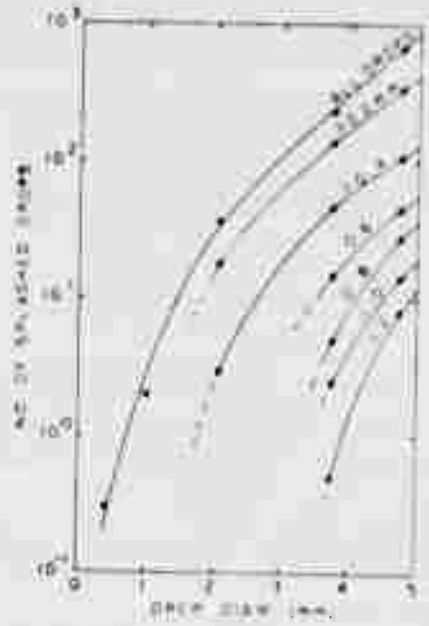

Fig. 8. The number of plashed drops > the indicated size, that are produced by the impact of a fresh-water drop on a sea water surface. As these data were obtained with the aid of filter papers, splashed drops < about 100 microns diameter and those remaining airborne (Curve B, Fig. 7) were not included.

entirely on the size and number of splashed drops it was necessary to determine the "splashed drop spectrum" over the range of raindrop size. This was done by catching the splashed drops on 60 × 90 cm squares of Whatman No. 1 filter paper. The "raindrops" and the sea water contained a sufficient amount of methylene blue dye to enable the splashed drops, at least down to about 100 μ diameter, to be recorded as a blue spot on the filter paper. Tensiometer measurements showed that the blue dye did not significantly change the surface tension, consequently the character of the splash would not be expected to change. The relation of drop size to spot size on the filter paper was determined by letting drops of known size fall on the papers. A semi-disc of 10 cm diameter was cut from the center of the 90 cm edge of the filter paper and the paper then placed about 5 mm above the sea water surface and so positioned that the water drops would splash at the edge of the paper at the center of the semicircular opening. Only half of the splash was recorded so the final count of drops on the filter paper was multiplied by two. The splash from the largest drops extended out to about 50 cm from the point of impact of the drop with the water. The splash from four to six drops in each of three size categories from 2—5 mm was counted. Figure 8 presents the data in the form of a family of curves showing the total number of splashed drops larger than the indicated size. It can be seen that nearly half of the splashed drops are < 0.2 mm. A raindrop of 5 mm might be expected to produce nearly 900 drops of a size that is detected on the filter paper, of which only about 400 exceed 0.2 mm and only 12 exceed 1.2 mm. The splash from raindrops < 2 mm is probably mainly composed of drops < 0.4 mm. Drops < 1 mm produce, on the average, less than one splash drop. These last splash observations were made visually.

It now remains to determine just what this splash means in terms of bubble production. It might be expected that the bubble-producing ability of the splash drops would be a function of their velocity and the angle at which they enter the water. A larger number of combinations may be met with in the splash of a single large drop but fortunately a simplification enables us to make a reasonable estimate of the bubble production. The splash drops are observed to rise up to 40 cm from the water surface, a height sufficient to insure that drops up to 0.5 mm will nearly attain terminal velocity by the time they return to the water surface. Figure 8 indicates that all the splash drops from raindrops < 2 mm and about 80 percent from a 5 mm raindrop are < 0.5 mm. We might reasonably expect then that the splash drops could be considered as raindrops and, as discussed earlier in this section, each produce 2—3 bubbles of about 50 μ diameter. On this basis the splash from a 2 mm raindrop might be expected to produce some 80 bubbles compared to over 2,000 for a 5 mm raindrop.

The third method of bubble production by raindrops falling into the sea is from "floating drops". These drops are similar to those that can be seen skimming across the surface of the water any time the water is violently agitated. As indicated in Fig. 6 the floating drops can be produced by both the splashed drops and the bubbles. Presumably the few that are produced by splashed drops are from drops that were not splashed to any great height while those produced by bubbles are presumably the lower, larger drops in the jet that is produced

when the bubble breaks. Observations on floating drops of about 2 mm diameter show that when they finally merge with the main body of water a thin column of bubbles is forced down several mm into the water. When these bubbles, perhaps 40 or more, fan out they are seen to be very small, perhaps $< 25\,\mu$ diameter. Little can be said of the numbers or sizes of these floating drops that are produced by raindrops. It may be that rain produces relatively few compared to those that may be produced by breaking waves.

The airborne salt nuclei produced by direct impact of the raindrops with the water are nothing more than splashed drops that are, for the most part, small enough to remain airborne. Drops of 4.7 mm were observed to produce an estimated several hundred particles of < about 50 microns diameter. At impact these particles seem to appear simultaneously within a region up to 4 cm above the water and some 10 cm from the point of impact. No doubt this is caused by the fact that the production mechanism of the particles gives them sufficient speed to escape detection by the eye until frictional retarding forces decrease their speed to the terminal value. This production mechanism appeared to be associated with the rapid formation and collapse of the large bubble that WORTHINGTON and COLE (1897) observed in their splash studies. In any event the ejection of the particles several cm above the surface increases the probability that they will remain airborne. Some of these particles were so small (< 10 microns) that a collection of them appeared and behaved like a small puff of smoke. There was no doubt that these would remain airborne, especially if the humidity were low over the water surface. The production of these minute splash drops was very much a function of drop size. A 2.4 mm drop produced perhaps 50—80 small particles while a 0.4 mm drop produced none that was visible to the naked eye (see Fig. 7).

D. Air Solubility Change in the Sea

The dissolved air content of the surface layers of the sea is usually at or near saturation and will vary from one season to the next. This seasonal change is presumably explained by the fact that the solubility of air in sea water is a function of temperature and also that the production or utilization of oxygen by marine organisms will vary with the seasons. As the solubility of air is an inverse function of temperature it follows that, at saturation values, a maximum would be found near the end of the winter months when the water is at its lowest temperature and a minimum at the end of summer when the water is warmest. Consequently air should be given off by the sea during the spring and summer and absorbed during the winter. REDFIELD (1948), after an analysis of the seasonal variations of the oxygen distribution in the Gulf of Maine, concluded that about 3×10^5 cc of oxygen leaves the sea through a m^2 of sea surface during March—October and a similar amount re-enters during the winter and spring. It is logical to inquire as to how much of this oxygen might leave the sea in the form of bubbles. If we go to extremes and assume that it all comes out in the form of bubbles of 50 microns diameter we can compute the rather staggering number of 2,500 bubbles sec^{-1} cm^{-2} breaking at the sea surface. This certainly does not occur, as gaseous diffusion across the sea surface probably accounts for the greater part of the oxygen exchange in the normal course of events. However an intriguing question is whether bubble formation occurs in the sea after a short period of intense heating by an overlying warm air mass. If supersaturation by heating can keep ahead of the loss by gaseous diffusion to the air, and if sufficient nuclei for centers of bubble formation exist, there is a possibility that bubbles may form. Inasmuch as little or nothing is known of the interplay between these factors little more can be said.

Precipitation falling into the sea may, under certain conditions, bring about a supersaturation of the rain water—sea water mixture, even though both were only saturated initially. As the inverse relation between air solubility and temperature is not linear but in the form of a curve concave upward, it follows that the mixing of two initially saturated bodies of water at different temperatures will produce a supersaturated mixture. For example, consider raindrops which have essentially the wet bulb temperature (KINZER and GUNN, 1951) and undoubtedly are saturated at that temperature. If raindrops, of a chlorinity essentially zero and saturated with air at 10° C, fall into saturated sea water (Cl = 19‰) at 24° C and

mix such that the mixture is 90 percent sea water, the resulting supersaturation will be about 102 percent[1]. Such supersaturations are probably not sufficient to cause bubble nucleation, but the rate of solution of the small bubbles produced by wave action and precipitation would be decreased. The important subject of the rates of solution of an air bubble as a function of saturation percentage will be discussed in the next section.

3. The Stability of Air Bubbles in Sea Water

The foregoing experiments have shown that whitecaps and all forms of precipitation particles are effective bubble producers. If these bubbles are produced in subsaturated water there is the possibility that a significant decrease in bubble diameter will be caused by the air within the bubble going into solution. On the other hand, if the water is sufficiently supersaturated many of the bubbles would be expected to grow. It will be clear shortly that for any supersaturation of sea water there exists a bubble size above which all bubbles will grow while those smaller than this size will go into solution. This modification of bubble size is clearly then a function of its initial size, the sea water saturation and the duration of existence of the bubble. Bubbles carried far beneath the surface will be subjected to gas diffusion across the bubble—water interface for considerably longer periods of time and are thus subject to greater change than those near the surface. Consequently it is very important that we obtain some knowledge of the effects of various solution times and rates on the bubble spectrum.

The calculations outlined here are an extension of those given by WYMAN ET AL (1952) and the reader should refer to these authors for a full understanding of the initial formulation. As a first approximation consider that due to the relative motion between the water and the bubble that the only gradient of dissolved gas that exists is across a thin shell with its inner surface at the air—water interface. Further assume that the air within the bubble consists of a single gas with a single diffusion constant and not primarily a mixture of oxygen and nitrogen. The general gas law states:

$$n = \frac{1}{RT}\,\frac{4}{3}\,\pi\, r^3 p \qquad (5)$$

when n is the number of moles of gas in the bubble; R, the gas constant; T, the absolute temperature; r, the radius of the bubble; and p, the pressure within the bubble. The pressure p is the hydrostatic plus the atmospheric pressure. The diffusion of air across the bubble surface can be expressed by Fick's law:

$$dn/dt = -\delta\, 4\,\pi\, r^2\,(p - p_0) \qquad (6)$$

where p_0 is the partial pressure of the air in the bulk water and δ is a constant defined by: $\delta = \triangle\, \alpha/d$ where $\triangle$ is the diffusion constant of the air in the water; α, the solubility of the air in the water, and d, the thickness of the thin shell that is assumed to carry the diffusion gradient. It will be seen that this expression is necessary to convert $(p - p_0)$ in (6) into a concentration gradient as called for in Fick's law. If we differentiate (5) with respect to time and combine it with (6) we have:

$$dr/dt = -\delta\, RT\,\frac{(p - p_0)}{p} \qquad (7)$$

This is the equation that was derived by WYMAN ET AL. (1952) and found to be in very good agreement with experiment. Experimentally they found that dr/dt at any given pressure was essentially constant, that it approached a limiting value at high pressures and it was essentially independent of temperature over the range 1—27° C. This is just what (7) predicts. As the water was always saturated with respect to air at one atmosphere, pressure p_0 is constant and dr/dt can be seen to approach a limiting value, $\delta\, RT$, at great depths. As the rate of solution is proportional to the absolute temperature dr/dt will change relatively little with the temperature range used in the experiments. With the experimental data one may compute the value of the term $\delta\, RT$ to be 10^{-4} cm sec^{-1} and find that it is approximately constant at all depths. Equation (7) with this substitution combines both theory and experiment to describe the rate of solution of gas bubbles.

It should be noted in (7) that the total pressure p within the bubble is assumed to be only the hydrostatic plus atmospheric pressure

[1] This calculation was based on tables of air saturation as a function of temperature and chlorinity as given by MIYAKE (1951).

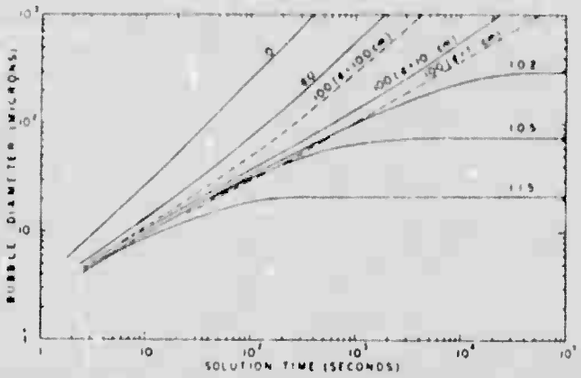

Fig. 9. The time of solution for a bubble in sea water at a depth of 10 cm. The family of curves represents various percentage saturations of air in sea water with respect to atmospheric pressure. The dashed lines show the solution times for bubbles at a depth of 1 and 100 cm in water saturated with air with respect to atmospheric pressure.

and no account is taken of the additional pressure $2\gamma/r$ due to surface tension effects (the surface tension of sea water γ is about 74 dynes cm^{-1}) This effect was negligible in the work of Wyman et al. where the bubbles were several mm in diameter but in the present case, where we must be concerned with bubbles < 100 microns, surface tension effects become of prime importance. If then we add the surface tension pressure term $2\gamma/r$ to the other pressure term p in (5) and (6) and solve simultaneously we obtain the general expression:

$$\int_0^t dt = -\frac{1}{3\delta RT}\int_{r^1}^{r^2}\frac{3pr+4\gamma}{r(p-p_0)+2\gamma}\,dr \qquad (8)$$

which reduces to (7), as it should, if γ is set equal to zero. The solution of this integral is:

$$t = -\frac{(p-p_0)^{-1}}{3\delta RT}\left[3pr+\gamma\right.$$

$$\left.\left\{\frac{4(p-p_0)-6p)}{p-p_0}\right\} ln\ \{(p-p_0)r+2\gamma\}\right]_{r^1}^{r^2} \qquad (9)$$

Figure 9 was constructed from (9) and shows the solution times for bubbles in water of various degrees of saturation at a depth of 10 cm. The dashed lines show the solution times in water saturated at atmospheric pressures at depths of 1 and 100 cm. Note that within these depths there is little significant difference in solution times in saturated water for bubbles < about 40 microns diameter. The significance in Figure 9 would seem to be the equilibrium bubble diameters that are indicated at each value of supersaturation, below which all bubbles will, due to surface tension pressure effects, go into solution. Even at a supersaturation of 115 % all bubbles < 21 microns will be forced into solution. The value of this equilibrium diameter may be very important for if the majority of bubbles in a given bubble spectrum are < this value, the bubbles themselves may be responsible for further increasing the supersaturation. As the supersaturation curves in Fig. 9 were constructed for a depth of 10 cm, it is of interest to determine how the equilibrium bubble diameters vary with depth as a function of supersaturation.

A bubble is at equilibrium with its surroundings when its total internal pressure, which is composed of the atmospheric, the hydrostatic and the surface tension pressures, is equal to the partial pressure of the gas in solution. As we are considering the case where the water is saturated at all depths with respect to atmospheric pressure, the partial pressure of the gas is xA, where x is the fractional value of the supersaturation and A is the atmospheric pressure. This is equated to the three components of the total internal pressure as given above to obtain

$$xA = A + d + \frac{2\gamma}{r} \qquad (10)$$

where d is the hydrostatic pressure. Solving for r we find

$$r = \frac{2\gamma}{(x-1)A - d} \qquad (11)$$

from which it is seen that for any supersaturation x there is a depth d beyond which all bubbles will go into solution. This depth is found by letting the denominator in (11) equal zero and solving for d. For supersaturations < 102 percent this depth is < 10 cm. At supersaturations > 102 percent (11) shows that for depths < 10 cm the critical radius, above which or below which bubbles grow or go into solution, is essentially constant for a given supersaturation and thus similar to the values indicated in Fig. 9. The time required for the bubbles to go into solution will decrease with depth in the range of 0—100 cm but probably not significantly so, judging from the curves for depth of 1 and 100 cm in Fig. 9.

4. Discussion

It will be of interest to examine the experimental data on the effectiveness of bubble production by breaking waves and precipitation in terms of the salt nuclei spectrum found in the atmosphere. The breaking wave is probably the most common method of production of airborne nuclei. With the data from Fig. 3 and Fig. 4 we can derive Table 1 which indicates the rate at which bubbles of various sizes rise to the surface cm^{-2} sec^{-1}. Assuming that only one of the 4 or 5 drops ejected from the breaking bubble remains airborne, column D of Table 1 can also represent the production rate of airborne nuclei from the sea surface shortly after a whitecap has formed. It would be unwise to attempt to compute the total production of nuclei from a breaking wave for we do not know to what depths the bubbles are carried and thus cannot say how long the concentration given in column B will be in existence. If the bubbles are all distributed uniformly to the same depth then the smallest ones will continue to break at the surface for the longest time. The production rate (column D) of about 34 cm^{-2} sec^{-1} is comparable to the value of 40 cm^{-2} sec^{-1} (for nuclei of mass > 10^{-13} g) found by MOORE and MASON (1954) in laboratory tests. It would be well to regard the similarity of these two values as probably fortuitous, and to accept it only as an agreement in order of magnitude. It is not clear as to whether bubbles were breaking over the entire area used in Moore and Mason's laboratory tests or only over a fraction of it. Also, it is not known how the present results will be affected by changes in wind force on the open sea. It is expected that increasing wind force will increase the numbers of bubbles in such a way that the slope of the curve in Fig. 4 will be essentially the same.

Table 1. An attempt to estimate the number of bubbles (cm^{-1} sec^{-1}) from a breaking wave. Columns B and C are obtained from Figs. 4 and 3, respectively. Column D is simply the product of B and C. Column E is obtained from D by assuming only 10 percent of the ocean active as a source bubbles.

A	B	C	D	E
Bubble diam. of center of size band (μ)	Bubbles cc^{-1} per 100 μ band width	Rise velocity cm sec^{-1}	Bubbles cm^{-1} sec^{-1}	Bubbles produced cm^{-1} sec^{-1} assuming 10 % of sea active
75	100	0,3	30	3
150	3,6	0,9	3,24	0,32
250	0,25	1,9	0,47	0,047
350	0,05	2,95	0,15	0,015

Probably the most significant aspect of Table 1 is that the great majority of the bubbles are < 200 μ. From Fig. 2 we see that these bubbles, upon bursting, could produce nuclei of the size found at the small end of the airborne sea-salt spectrum (< about 10^{-10} g) by drops from the jets. MOORE and MASON (1954), with doubts as to the existence of bubbles < about 500 μ from whitecaps, have suggested that airborne salt nuclei < 10^{-9} g originate from the shattering of the film of the large bubbles. Inasmuch as the small bubbles do indeed exist it is likely that the mechanism by which the nuclei are produced is via the jet mechanism and not the bubble film. Observation (BLANCHARD 1954) shows that small bubbles (< 50 μ) produce no droplets exceeding 1 μ radius, other than those coming from the jet mechanism. MASON (1954) reports that bubbles of 0.5 to 3 mm give 100—200 droplets from the shattered film, with the largest having salt contents of about 2×10^{-14} g. This weight is far less than the minimum of about 10^{-10} g that appears to provide the

nuclei for raindrop formation (WOODCOCK and BLANCHARD 1955).

The entire question as to the spectrum of bubbles that produce these large airborne nuclei and the exact method by which it is done may appear to be a trivial one. And it could well be so, if we were to assume that the properties of two drops of equal size, one produced by the jet mechanism and the other by the rupture of the bubble film, were the same. But this may not necessarily be so. It has been found (BLANCHARD 1955) that the droplets arising from the jet mechanism carry an appreciable electric charge that may contribute significantly to electrification processes in the atmosphere. Other considerations indicate that the droplets that are created by the jets may not be representative of the bulk sea water but of the surface film which may be contaminated. If droplets arising from the rupture of bubble films do not have the aforementioned properties they may play a different role in the precipitation process than those arising from the jet mechanism.

The production of bubbles by falling snow was found to be about 25 cm^{-2} sec^{-1} which, again assuming one airborne droplet per bursting bubble, gives a salt nuclei production rate of the same value. This is to be compared to the somewhat similar computed value of about 14 found for the nuclei production from bubbles produced by rain. The nuclei production by rain was estimated by carrying out the following steps, with each of the raindrop size distributions given by BLANCHARD (1953) and BEST (1950) for rain intensities of 20.8 and 25 mm hr^{-1}, respectively. Each distribution was divided into a number of intervals ($\leq 250\,\mu$) and the number of drops striking the sea cm^{-2} sec^{-1} was computed. Then by using Fig. 7 and Fig. 8 one could compute the production rate of airborne nuclei from (a); bubbles produced directly by the drop, (b); impact of the drop and (c); bubbles produced by the drops < 0.4 mm that were splashed by the raindrops. It was found that the bubbles produced at impact were responsible for more than 80 percent of the total airborne nuclei and, even more surprising, Blanchard's rain distribution above (all drops ≤ 2.2 mm) produced about as many bubbles as did Best's (drops as large as 5 mm). It appears that the greater number of drops m^{-3} in the narrow range distribution made up for the fact that larger drops produce more bubbles. These data indicate that a significant increase in the salt nuclei count might be found in atmospheric regions overlying the ocean through which rain or snow had fallen. The build up of airborne nuclei in such regions would be a function of the wind shear between sea level and the precipitation source and the duration of the precipitation.

The question as to the production of bubbles by the warming of the sea in the summer months or by the mixing of two saturated water masses at different temperatures will, as mentioned earlier, have to await more observations on the supersaturations of surface waters of the sea. The existence of supersaturations will depend, in some degree, on the absence of bubble nuclei. In the absence of these nuclei, which are thought to be gas particles surrounded by minute foreign materials in the water, the water may be highly supersaturated without the formation of bubbles (DEAN, 1944). The idea was recently advanced (FOX and HERZFELD, (1954) than minute bubbles in water, which are prevented from going into solution by the stabilizing action of an organic skin, will act as cavitation nuclei. They envisaged that this organic skin, probably produced by the disintegration of living organisms, acted as a mechanical barrier to the diffusion of gases. Upon cavitation the organic skin could be torn and bubble growth would follow. It seems probable that such bubble nuclei could exist in the oceans but their importance in bubble production in natural supersaturated waters is unknown.

From the calculations presented in Section 3 it appears that supersaturations in the surface layers of the sea can be produced by the small bubbles that are forced into solution by the increase in internal bubble pressure due to surface tension. Figure 9 indicates that supersaturation of at least 102 percent could occur if the bubbles are $< 300\,\mu$ diameter. As the results of Section 2 show that a majority of the bubbles produced by natural processes are $< 300\,\mu$, it is to be expected that a slight supersaturation of the surface waters would be produced. In particular, as the majority of the bubbles produced by snowflakes are $< 50\,\mu$ diameter, it is expected that supersaturations of about 105 percent could be obtained. The

bubbling process will certainly produce supersaturations, as RAKESTRAW and EMMEL (1938) have measured nitrogen supersaturations of 102 percent in water that had been vigorously shaken with air and let stand until the bubbles were no longer visible.

If we assume that the usual saturation percentage at the sea surface is from 100 to 102, then in either case all bubbles $< 300\ \mu$ will tend to go into solution and at rates, at least for the bubbles < about $100\ \mu$, that are nearly the same. The solution rates for the larger bubbles, though significantly different for 100 and 102 percent saturation, need not be considered, for the rate of rise of these bubbles will bring them to the surface long before any appreciable decrease in diameter has taken place. The small bubbles, with rates of rise of only a few tenths of a cm sec^{-1}, will require several hundred or only a few seconds to reach the surface depending on whether they rise from depths of about a meter or a few cm, respectively. In the former case the bubble may go entirely into solution while in the latter little change in size may be experienced. It appears then that the depth to which a small bubble is carried may be an important factor in controlling the final bubble size. This depth, in turn, will be a function of the stability of the surface layers of the sea and the intensity of the mixing process. For example, we would expect very little downward mixing of bubbles produced by snow falling into a fairly calm sea. On the other hand, a great deal of downward mixing of bubbles from snow is to be expected in strong winds or when the surface waters are convectively unstable.

It is clear that many factors must be considered in order to make broad generalizations on the rate of nuclei production from naturally-produced breaking bubbles. Not only must we consider the various bubble producing mechanisms discussed in this paper, but we also must take into account the stability change of the surface layers of the sea as it varies geographically and with the seasons.

Acknowledgments

The writers would like to thank Mr. A. T. Spencer for his help in carrying out the experiments with simulated raindrops. They gratefully acknowledge the work of Mr. E. Florence on the bubble spectrum from breaking waves. Their former colleague, Dr. C. H. Keith, did all the work relating the bubble size to the mass and height of the ejected drops.

REFERENCES

ALIVERTI, G., and G. LOVERA, 1939: I fenomeni meteorologici sull'Oceano e il campo elettrico terrestre. *Atti della Reale Accademia delle Scienze di Torino* **74**, pp. 573—590.

ALLEN, H. S., 1900: The motion of a sphere in a viscous fluid. *Phil. Mag.*, **50**, pp. 323—338.

BEST, A. C., 1950: The size distribution of raindrops. *Quart. J. Roy. Met. Soc.*, **76**, pp. 16—36.

BLANCHARD, D. C., 1953: Raindrop size-distribution in Hawaiian rains. *J. Met.*, **10**, pp 457—473.

— 1955. Electrified droplets from the bursting of bubbles at an air—sea water interface. *Nature*, **175**, pp. 334—336.

— 1954: Bursting of bubbles at an air-water interface. *Nature* **173**. p. 1048.

BOWEN, E. G., 1950: The formation of rain by coalescense. *Australian J. of Sci. Res.*, **3**, pp. 193—213.

BOYCE, S. G., 1951: Source of atmospheric salts. *Science*, **113**, pp. 620—621.

BYERS, H. R., 1955: Distribution in the atmosphere of certain particles capable of serving as condensation nuclei. *Proc. Conf. Physics of Cloud and Precip. Particles*, Woods Hole Ocean. Inst., Woods Hole, Mass. To be publ.

COSTE, J. H., and H. L. WRIGHT, 1935: The nature of the nucleus in hygroscopic droplets. *Phil. Mag.*, **20**, pp. 209—234.

CROZIER, W. D. and B. K. SELLY, 1950: Some techniques for sampling and identifying particulate matter in the air, *Proceeding of First National Air Pollution Symposium*, p. 45, Stanford, Calif., Stanford Press.

DEAN, R. B., 1944: The formation of bubbles. *J. App. Physics* **15**, pp. 446—451.

FOURNIER D'ALBE, E. M., 1951: Sur les embruns marins. *Bull. Inst. Oceanogr., Monaco*, **48**, No. 995, 7 pp.

FOX, F. E. and K. F. HERZFELD, 1955: Gas bubbles with organic skins as cavitation nuclei. *J. Acoust. Soc. of Amer.* **26**, pp. 984—989.

GOLDSTEIN, S., 1938: *Modern developments in fluid dynamics*. Vol. 1, p. 14. Oxford at the Clarendon Press.

KIENTZLER, C. F., A. B. ARONS, D. C. BLANCHARD, and A. H. WOODCOCK, 1954: Photographic investigation of the projection of droplets by bubbles bursting at a water surface. *Tellus*, **6**, pp. 1—7.

KINZER, G. D., and R. GUNN, 1951: The evaporation, temperature and thermal relaxation-time of freely falling waterdrops. *J. Met.*, **8**, pp. 71—83.

KNELMAN, F., N. DOMBROWSKI, and D. M. NEWITT, 1954: Mechanism of the bursting of bubbles. *Nature* **173**, p. 261.

KÖHLER, H., 1941: An experimental investigation on sea water nuclei. *Nova Acta reg. Soc. Sci. Upsaliensis*, ser. 4, **12**, No. 6, 55 pp.

LUDLAM, F. H., 1951: The production of showers by the coalescence of cloud droplets. *Quart. J. Roy. Met. Soc.*, **77**, pp. 402—417.

MASON, B. J., 1954: Bursting of bubbles at the surface of sea water. *Nature*, **174**, pp. 470—471.

MIYAKE, Y., 1951: The possibility and the allowable limit of formation of air bubbles in the sea. *Papers in Meteorology and Geophysics*, **2**, pp. 95—101.

MOORE, D. J., 1952: Measurements of condensation nuclei over the North Atlantic. *Quart. J. Roy Met Soc.*, **78**, pp. 596—602.

MOORE, D. J., and B. J. MASON, 1954: The concentration, size distribution and production rate of large salt nuclei over the oceans. *Quart. J. Roy. Met. Soc.*, **80**, pp. 583—590.

OWENS, J. S., 1926: Condensation of water from the air upon hygroscopic crystals. *Proc. Roy. Soc., London*, A, **110**, pp. 738—752.

RAKESTRAW, N. W., and W. M. EMMEL, 1938: The solubility of nitrogen and argon in sea water. *J. Phys. Chem.*, **42**, pp. 1211—1215.

REDFIELD, A. C., 1948: The exchange of oxygen across the sea surface. *J. Mar. Res.*, **7**, pp. 347—361.

STUHLMAN, O., 1932: The mechanics of effervescence. *Physics*, **2**, pp. 457—466.

TWOMEY, S., 1955: The distribution of sea-salt nuclei in air over land. *J. Met.*, **12**, pp. 81—86.

WOODCOCK, A. H., 1948: Note concerning human respiratory irritation associated with high concentrations of plankton and mass mortality of marine organisms. *J. Mar. Res.*, **7**, pp. 56—62.

WOODCOCK, A. H., and MARY M. GIFFORD, 1949: Sampling atmospheric sea-salt nuclei over the ocean. *J. Mar. Res.*, **8**, pp. 177—197.

WOODCOCK, A. H., 1952: Atmospheric salt particles and raindrops. *J. Met.*, **9**, pp. 200—212.

— 1953: Salt nuclei in marine air as a function of altitude and wind force. *J. Met.*, **10**, pp. 362—371.

WOODCOCK, A. H. and D. C. BLANCHARD, 1955: Tests of the salt-nuclei hypothesis of rain formation. *Tellus*, **8**, pp. 437—448.

WORTHINGTON, A. M., and R. S. COLE, 1897: Impact with a liquid surface, studied by the aid of instantaneous photography. *Phil. Trans.*, **189** A, pp. 137—148.

WRIGHT, H. L., 1940: Atmospheric opacity at Velentia. *Quart. J. Roy. Met. Soc.*, **66**, pp. 66—77.

WYMAN, JR., J., P. F. SCHOLANDER, G. A. EDWARDS, and L. IRVING, 1952: On the stability of gas bubbles in sea water. *J. Mar. Res.*, **11**, pp. 47—62.

PRINTED IN SWEDEN
ESSELTE, STHLM 57